



Published in final edited form as:

*Nat Commun.* ; 5: 5190. doi:10.1038/ncomms6190.

## Integrated Control Of Hepatic Lipogenesis Vs. Glucose Production Requires FoxO Transcription Factors

Rebecca A. Haeusler<sup>1,2</sup>, Kirsten Hartil<sup>3</sup>, Bhavapriya Vaitheesvaran<sup>3</sup>, Isabel Arrieta-Cruz<sup>3</sup>, Colette M. Knight<sup>3</sup>, Joshua R. Cook<sup>2</sup>, Helene L. Kammoun<sup>4</sup>, Mark A. Febbraio<sup>4</sup>, Roger Gutierrez-Juarez<sup>3</sup>, Irwin J. Kurland<sup>3</sup>, and Domenico Accili<sup>2</sup>

<sup>1</sup>Department of Pathology and Cell Biology, Columbia University, New York, NY

<sup>2</sup>Department of Medicine, Columbia University, New York, NY

<sup>3</sup>Department of Medicine, Albert Einstein University, Bronx, NY

<sup>4</sup>Cellular and Molecular Metabolism Laboratory, Baker IDI Heart and Diabetes Institute, Melbourne, Victoria, Australia

### Abstract

Insulin integrates hepatic glucose and lipid metabolism, directing nutrients to storage as glycogen and triglyceride. In type 2 diabetes, levels of the former are low and the latter are exaggerated, posing a pathophysiologic and therapeutic conundrum. A branching model of insulin signaling, with FoxO1 presiding over glucose production and Srebp-1c regulating lipogenesis, provides a potential explanation. Here we illustrate an alternative mechanism that integrates glucose production and lipogenesis under the unifying control of FoxO. Liver-specific ablation of three FoxOs (L-FoxO1,3,4) prevents the induction of glucose-6-phosphatase and the repression of glucokinase during fasting, thus increasing lipogenesis at the expense of glucose production. We document a similar pattern in the early phases of diet-induced insulin resistance, and propose that FoxOs are required to enable the liver to direct nutritionally derived carbons to glucose vs. lipid metabolism. Our data underscore the heterogeneity of hepatic insulin resistance during progression from the metabolic syndrome to overt diabetes, and the conceptual challenge of designing therapies that curtail glucose production without promoting hepatic lipid accumulation.

---

Users may view, print, copy, and download text and data-mine the content in such documents, for the purposes of academic research, subject always to the full Conditions of use:[http://www.nature.com/authors/editorial\\_policies/license.html#terms](http://www.nature.com/authors/editorial_policies/license.html#terms)

#### AUTHOR CONTRIBUTIONS

R.A.H. designed and performed experiments, analyzed data and wrote the manuscript. K.H., B.V., I.A.-C., C.M.K., H.L.K., and R.G.-J. designed and performed experiments and analyzed data. M.A.F., I.J.K. and D.A. designed experiments, analyzed the data and wrote the manuscript.

#### COMPETING FINANCIAL INTERESTS

The authors declare no competing financial interests.

#### Accession codes

Microarray data have been deposited in Gene Expression Omnibus under accession code GSE60527.

## Introduction

The integrative regulation of hepatic carbohydrate and lipid metabolism by insulin is a key biological question with important ramifications for the pathogenesis and potential treatment of type 2 diabetes (T2D)<sup>1</sup>. Diabetics overproduce glucose and triglycerides, contributing to the twin abnormalities of this disease, hyperglycemia and hypertriglyceridemia<sup>2</sup>. Less clear is how these actions of insulin are mediated, and why they are inextricably linked in the pathogenesis of insulin resistance, the forerunner of T2D.

Insulin's repression of hepatic glucose production (HGP)<sup>2</sup> is mediated by the Irs–Akt–FoxO pathway<sup>3–7</sup>. Conversely, insulin promotes de novo lipogenesis (DNL), through Akt-mediated activation of Srebp-1c<sup>8–10</sup>. A widely held model suggests that insulin signaling bifurcates downstream of Akt, to regulate HGP and DNL separately, through these two independent, parallel effectors<sup>1</sup>. In contrast to this model, evidence suggests that FoxOs are also required for normal regulation of lipid synthesis and metabolism<sup>6,11–16</sup>.

FoxOs are thought to promote HGP primarily by activating transcription of glucose 6 phosphatase (encoded by *G6pc*)<sup>2</sup>. However, there are two problems with this explanation: first, *G6pc* enzyme levels are at best modestly correlated with HGP in diabetes<sup>17</sup>; and second, the effect of liver FoxO ablation on HGP vastly exceeds its effect on *G6pc*<sup>3,5,7</sup>. Moreover, mice with a triple knockout of Akt1/Akt2/FoxO1 in liver (or Irs1/Irs2/FoxO1) have a transcriptional response to fasting and refeeding (F–RF) that is similar to controls<sup>4,5</sup>, raising the question of whether and how FoxOs are required for the F–RF response.

We expected that a major reason for the mild defects observed after FoxO1 knockout is the redundancy of FoxOs<sup>3,5</sup>. We employed a combination of genetic, metabolomic, and flux analysis in L–FoxO1,3,4 mice to address two goals: (i) to critically test the model that FoxOs promote HGP but do not regulate DNL; and (ii) to examine the requirement for FoxOs during the F–RF transition in healthy mice. We report that FoxOs exert dual control over *G6pc* and *glucokinase* (*Gck*), thus determining whether glucose-6-phosphate is routed toward glucose vs. lipid metabolism.

## Results

### Hepatic FoxOs control the G6pc/Gck ratio

We found that 30% of L–FoxO1,3,4 mice die prior to weaning (Fig. 1a), possibly due to fatal postnatal hypoglycemia (Supplementary Fig. 1a)<sup>7</sup>. Surviving adult L–FoxO1,3,4 mice presumably have the most robust compensatory mechanisms, but still showed low glucose and insulin during day time *ad libitum* feeding, and hypoglycemia after prolonged fasting (Supplementary Fig. 1b–c)<sup>7,18</sup>. In hyperinsulinemic–euglycemic clamps, L–FoxO1,3,4 mice required double the glucose infusion rate of controls (Fig. 1b). There was no significant difference in glucose disposal, but L–FoxO1,3,4 mice showed ~60% reduction in HGP (Fig. 1c–d).

We investigated transcriptional mechanisms of metabolic control by FoxO during fasting and refeeding (F–RF). In controls, *G6pc* peaked at 4 hr of fasting, but L–FoxO1,3,4 mice

were unable to induce this peak (Fig. 1e). Consistent with this, fasting L-FoxO1,3,4 mice showed delayed glycogen depletion (Fig. 1f). *Igfbp1*—a canonical FoxO target—showed an expression pattern similar to *G6pc*, but there was no defect in the expression of *Pck1* in L-FoxO1,3,4 mice (Supplementary Fig. 1d–e). We unexpectedly identified a 40% decrease in expression of the glucose 6-phosphate transporter (Fig. 1g). Thus, this transporter may contribute to FoxO's control of glucose release from liver<sup>19</sup>, although it was not strongly regulated by F-RF.

Next we measured expression of glucokinase (encoded by *Gck*), which is critical for hepatic glucose utilization<sup>20–27</sup>, and is negatively regulated by FoxOs<sup>7,15,18,28</sup>. In controls, *Gck* was strongly suppressed during fasting, and induced within 1-hr of RF (Fig. 1h). In contrast, in L-FoxO1,3,4 mice, *Gck* was hardly suppressed during fasting. Notably, *Gck* expression in L-FoxO1,3,4 mice fasted for 24 hr was similar to controls RF for 1hr, demonstrating that inactivating FoxOs mimics the early effect of refeeding on *Gck*.

Because *G6pc* opposes *Gck* to control the intracellular gradients of glucose and glucose-6-phosphate, the ratio of the two enzymes may reflect the direction of glucose flux. In control mice, the *G6pc/Gck* ratio was potently induced during fasting, consistent with increased hepatic glucose output, but this effect was completely absent in L-FoxO1,3,4 mice (Fig. 1i). Furthermore, the ratio of *G6pc/Gck* was the strongest predictor of glycemia in L-FoxO1,3,4 pups ( $R = 0.75$ ) ( $P = 0.0001$ ) (Fig. 1j). This was not true in control pups, which showed nearly undetectable *Gck*, as expected<sup>29–31</sup>. This suggests that *G6pc* is only rate-limiting in the presence of counteraction by *Gck*. Analyzed individually, *Gck* was less strongly correlated to glucose, as was *G6pc* (Supplementary Fig. 1f–g).

To buttress the conclusion that FoxOs are important for regulation of the transcriptional response F-RF, we performed unbiased surveys of expressed mRNAs. Analyses of global gene expression patterns after 22 hr fasting or 4 hr RF revealed that fasted L-FoxO1,3,4 mice largely resemble RF controls (Supplementary Fig. 1h). This demonstrated that inactivating FoxOs mimics the effect of RF on a large portion of nutritionally regulated genes. Finally, we confirmed that FoxOs are required for induction of *G6pc* and suppression of *Gck* using primary hepatocytes derived from control or L-FoxO1,3,4 mice (Supplementary Fig. 1i).

### Glucose cycling and *de novo* lipogenesis in FoxO-deficient mice

To investigate glucose uptake and utilization, we injected mice with a mixture of two stable isotope-labeled glucoses<sup>32</sup>. In control mice, both tracers peaked in blood 30 min after injection and were cleared within 2-hr (Fig. 2a–b). At every time point, both tracers were reduced in L-FoxO1,3,4 mice (Fig. 2a–b), demonstrating increased glucose uptake and utilization. This can likely be attributed to liver, because glucokinase activators increase liver glucose uptake and glycolysis<sup>33</sup>, and because the rate of glucose disposal in the clamp (primarily reflecting glucose uptake in muscle and fat) showed no significant difference. Total plasma glucose and insulin were reduced in L-FoxO1,3,4, as expected<sup>7</sup> (Supplementary Fig. 2a–c). However, the fractional difference in enrichment of the two labels was the same in both genotypes (Fig. 2c), indicating no difference in the rate of glucose cycling<sup>34</sup>.

Increased Gck is expected to increase DNL<sup>23,24,35</sup>, and we next measured the rate of DNL during F–RF. In control mice, DNL was low after an 18 hr fast and quadrupled after 5 hr RF, but L–FoxO1,3,4 mice showed 2–3 times higher rates of DNL at both time points (Fig. 2d). We noted that DNL in 18-hr-fasted L–FoxO1,3,4 mice was nearly as high as in 5-hr-refed controls, indicating that FoxO inactivation mimics the effect of 5 hr refeeding on lipogenesis.

We next investigated lipogenic pathways that could explain the increased DNL. During prolonged fasting (when L–FoxO1,3,4 mice have ~3x higher DNL), we found no difference between genotypes in mRNA expression of target genes of canonical lipogenic transcription factors Srebp–1c and Chrebp, including *Acaca*, *Fasn*, *Elovl6*, and *Pklr* (Fig. 2e). Thus increases in Srebp–1c or Chrebp function cannot explain the increased lipogenesis in L–FoxO1,3,4 mice, while increased Gckcan (Fig. 2e–f).

Metabolomic and lipidomic analyses revealed that L–FoxO1,3,4 livers had increased G6P, pyruvate, triglycerides, and diglycerides (Fig. 2g–h, Supplementary Table 1), consistent with increased glycolysis and lipogenesis. Other metabolites showed no significant differences, except a trend towards reduced malate, potentially indicating that TCA cycle flux is preferentially re–routed into lipogenesis. The increased diglycerides were surprising, as they’ve been suggested to engender insulin resistance<sup>36</sup>, and L–FoxO1,3,4 mice are exceedingly insulin–sensitive.

Our data suggests that derepression of Gck may be an exquisitely insulin-sensitive mechanism to activate DNL<sup>23,24,35</sup> independently of canonical lipogenic pathways. We examined this in more detail in C57BL/6J mice during F–RF. Both *Elovl6* (Srebp–1c target) and *Pklr* (Chrebp target) were reduced during fasting and increased after refeeding, as expected (Fig. 3a). In contrast, the fluctuations of *Gck* were greater during F–RF, and peaked within 1–hr of refeeding, hours before Srebp–1c and Chrebp targets. We confirmed that Gck protein was induced within 1 hr of refeeding (Supplementary Fig. 3a).

### Alternative model of insulin control of hepatic glucose vs. lipid metabolism

Our data demonstrate that FoxOs regulate both glucose and lipid production, and suggests a new model of insulin’s regulation of these two processes. Instead of parallel functions through FoxOs and Srebp–1c, we propose that insulin acts on them sequentially (Fig. 3b): first, hepatic FoxOs are inactivated, immediately inducing glucokinase. In combination with glucose–dependent dissociation of Gck from its regulatory protein, this amplifies lipogenesis. Second, the Srebp–1c pathway is activated, thereby enhancing DNL. Our model is supported by the fact that FoxOs are inactivated within seconds of exposure to physiologic (picomolar) insulin doses, whereas Srebp–1c activation requires hours and higher insulin doses<sup>37</sup>. This proposed model justifies detailed future investigation of the time course of postprandial induction of DNL. Moreover, it may be worth investigating whether FoxOs’ dual effects on HGP and DNL are complementary to the effects of Hdac3 on hepatic metabolic routing<sup>38</sup>.

To investigate the pathophysiologic implications of this model, we examined the effects of one week of western–type diet (WTD) feeding in C57BL/6J mice. This dietary challenge

induced mild insulin resistance, as demonstrated by elevated glucose and insulin (Fig. 4a–b). This was associated with milder induction of *G6pc* and considerable blunting of *Gck* suppression during fasting (Fig. 4c–d). We confirmed that glucokinase protein was also increased in WTD–feeding (Supplementary Fig. 3b). Furthermore, WTD–fed mice showed marked decreases in the *G6pc/Gck* ratio during fasting (Fig. 4e). These data demonstrate that short–term WTD feeding mimics FoxO loss–of–function.

## Discussion

Key novel conclusions of this work are: (i) FoxOs are required for the dynamic regulation of *G6pc/Gck* during F–RF; (ii) this reciprocal regulation is a critical step in controlling hepatic glucose output and DNL; and (iii) short term WTD–feeding induces a phenotype resembling liver FoxO inactivation. Data presented in this study suggest a new model of glucose and lipid dysregulation in the pathophysiology of insulin resistance, based on successive defects in insulin action (Fig. 4f): in mild/early insulin resistance, portal hyperinsulinemia drives FoxO inactivation. This leads to a decrease in the *G6pc/Gck* ratio and excess DNL at the expense of hepatic glucose output. As the disease advances, there is a further rise in insulin and glucose levels, leading to induction of Srebp–1c/Chrebp–dependent lipogenesis. In this severe disease setting, FoxOs can be reactivated through oxidative stress<sup>39,40</sup> or an adverse kinase profile favoring their nuclear retention<sup>41</sup>.

This model, while partly still speculative, reconciles our molecular understanding of hepatic insulin signaling with the known clinical features of diabetes progression. Thus, in the early phases of the disease, hyperglycemia is mostly postprandial, but liver steatosis is already present<sup>42</sup>. In the advanced disease, fasting hyperglycemia accounts for a growing fraction of total glycemic variation<sup>43</sup>. In this setting, the combination of active transcription factors heralds the increase in both HGP and lipogenesis that is typical of the diabetic state.

Our data also help reinterpret studies showing that hepatic insulin signaling occurs normally in the absence of Akt1/Akt2/FoxO1 (Ref. <sup>5</sup>) or Irs1/Irs2/FoxO1 (Ref. <sup>4</sup>). We show that the gene expression profile of fasted mice lacking the three FoxOs is strikingly similar to that of fed wild type controls. This, in addition to the early postnatal death of a fraction of triple knockouts, and the profound flux abnormalities described in the survivors, should disabuse us of the notion that the FoxOs can be done away with. First, we suggest that the combined knockouts of Akt or Irs with FoxO1 didn't account for the functions of FoxO3a and 4, which we show to be substantial. Second, the ability of insulin to suppress HGP in clamp studies of Akt1/Akt2/FoxO1 mutants, which we confirm in triple FoxO knockouts in the present study, likely reflects two things: (1) the extra–hepatic actions of insulin, *e.g.* through FFAs or the CNS<sup>2</sup>; and (2) the contrived conditions of the clamp, wherein insulin levels are raised many fold over the physiologic range.

The novel models of insulin–FoxO regulation of HGP and DNL in normal physiology (Fig. 3b) and in the pathophysiology of diabetes (Fig. 4f) underscore the conceptual advances arising from this work. These findings should prompt a reappraisal of the heterogeneity of hepatic insulin resistance during the transition from the metabolic syndrome to overt

diabetes. They also provide a powerful illustration of the conceptual and regulatory challenges underlying the development of new treatments for this condition.

## METHODS

### Mice and diets

L-FoxO1,3,4 mice have been described<sup>7</sup>. Only males at least 16 weeks old were studied, except in studies of 2-day old pups, where pups of both genders were used. Male C57BL/6J mice were purchased from Jackson Labs and were studied at 9 weeks old. All mice were fed chow, except the experiment shown in Figure 4a–e, where C57BL/6J mice were challenged with WTD for one week. WTD is from Harlan Teklad (TD.88137); it contains approximately 30% kcal from sucrose and 42% from fat, and causes insulin resistance.<sup>12</sup> Mice were maintained on a 12-hour light–dark cycle (lights on at 7 am). The Columbia University Institutional Animal Care and Utilization Committee approved all experiments.

### Metabolic tests

Blood glucose was measured using One Touch glucose monitor and strips (Lifescan). Insulin ELISAs were from Millipore. Hyperinsulinemic–euglycemic clamps were carried 5–6 hours after removing food. We infused a solution of glucose (10%) at a variable rate to maintain plasma glucose ~8 mM. Mice received a constant infusion of [3-<sup>3</sup>H] glucose (0.1 mCi/min) and insulin (3.6 mU/kg body weight/min). We collected plasma samples to determine glucose levels at times 10, 20, 30, 40, 50, 60, 70, 80, and 90 minutes after beginning insulin and glucose infusions, and measured the specific activities of [3-<sup>3</sup>H] glucose and <sup>3</sup>H water at 40, 50, 60, 70, 80, and 90 minutes after beginning the insulin and glucose infusions. We achieved steady-state conditions for plasma glucose concentration and specific activity within 40 minutes from the beginning of the insulin clamp. During the last 10 minutes of the clamp study, we infused a solution of [U-<sup>14</sup>C] lactate in normal saline (5 μCi as initial bolus, followed by 0.25 μCi/min). At the end of the *in vivo* studies, mice were anesthetized, abdomens were quickly opened, portal blood was collected, and livers were freeze-clamped *in situ* and stored at –80°C for further analysis.<sup>44</sup> Hepatic recycling glucose tolerance tests (HR–GTTs) were carried out using a mixture of [2-<sup>2</sup>H] glucose (0.5 mg/g body wt) and [6,6-<sup>2</sup>H<sub>2</sub>] glucose (0.5 mg/g). When [2-<sup>2</sup>H]- and [6,6-<sup>2</sup>H<sub>2</sub>] glucose are administered as a 1:1 mixture, the disappearance of the two isotopes [2-<sup>2</sup>H]- and [6,6-<sup>2</sup>H<sub>2</sub>] glucose can be determined by mass fragmentography. The difference between the two disappearance rates is used to measure futile cycling. During the HR–dGTT, hepatic uptake of [2-<sup>2</sup>H] glucose generally leads to the loss of deuterium label at the C2 position due to isomerization between glucose-6-P and fructose-6-phosphate<sup>32</sup>. To measure *de novo* lipogenesis (DNL)<sup>45</sup>, following IP injection of deuterated saline, drinking water was replaced with 6% D<sub>2</sub>O. Following a 1-hr equilibration period, mice were either refed chow and sacrificed 5-hr later, or remained fasting for 18 hr. Newly synthesized palmitate was measured using GC–MS<sup>46</sup>. For time course studies in control vs. L-FoxO1,3,4, mice (shown in Figs. 1e–i), mice were first synchronized by removing food during daytime (10 am – 5 pm), then food was replaced at 5 pm. The experimental fasting period began at 7 pm. Mice were sacrificed at time 0 (*n* = 5 control; 5 L-FoxO1,3,4); 1-hr fast (*n* = 6 control; 5 L-FoxO1,3,4); 4-hr fast (*n* = 6 control; 4 L-FoxO1,3,4); 24-hr fast (*n* = 6 control, 4 L-

FoxO1,3,4); 1-hrrefed ( $n = 6$  control, 4 L-FoxO1,3,4). For time course studies in C57BL/6J mice (shown in Figs. 3a and 4a–e), the experiment was performed the same way, except the experimental fasting period began at 8 pm.

### Glycogen measurement

Tissue was homogenized in 6% perchloric acid and centrifuged at  $13,000 \times g$  for 10 min at 4 degrees C. The supernatant was combined with an equal volume of distilled water and centrifuged at  $13,000 \times g$  for 10 min at 4 degrees C. The supernatant was neutralized to pH 7 with KOH, centrifuged at  $13,000 \times g$  for 10 min at 4 degrees C, and the supernatant was incubated with amyloglucosidase at 42 degrees C for 2 hours. Released glucose was quantified using a glucose assay kit (Sigma, GAHK20).

### mRNA and protein expression

Liver RNA was prepared using Trizol, cDNA was synthesized using qScript (Quanta), and quantitative PCR was performed using goTaq (Promega). Primer sequences are available in Supplementary Table 2. Western blots used the primary antibodies directed against the following proteins: Gck (a kind gift from Mark Magnuson) was used at a 1:1,000 dilution, and actin (Abgent #AM1829b) was used at 1:5,000. Westerns were quantitated using Image J.

### Metabolomics

Liver tissue samples from fasted/re-fed experiments were extracted in ice-cold methanol/water (1:1)<sup>46</sup>. The relative concentrations of each metabolite were calculated using the area under the peak of M0 (unlabeled target ion) normalized to the internal standard and tissue weight.

### Lipidomics

Liver tissue samples were collected after 5-hr daytime fast. Lipid analysis was performed by liquid chromatography, electrospray ionisation-tandem mass spectrometry (LC ESI-MS/MS)<sup>47</sup>.

### Microarray analyses

We used GeneChip Mouse Exon arrays (Affymetrix) and Partek Genomics Suite software. For heat map analysis, we used the criteria of false discovery rate  $< 0.1$ .  $n = 3$  per group.

### Primary hepatocytes

Isolated primary hepatocytes were plated in Medium 199 + 10% FBS. Cells were serum-starved overnight in Medium 199 + 1% BSA. After overnight starvation, appropriate cells were pretreated with 100 nM insulin for 1 hour. Then, all cells were changed into serum-free medium containing (i) water + vehicle (EtOH); (ii) 0.1 M CPT-cAMP + 1 $\mu$ M dexamethasone; or (iii) cAMP/dex + 100 nM insulin. Cells were incubated for 6 hours in the treatment media, then harvested.

## Statistics and general methods

Sample sizes were estimated from expected effect size based on previous experiments. No randomization was used. One mouse was excluded from analysis in the DNL experiment, as it had an unclear genotype. Four mice were excluded from the HR–GTT analysis, due to problems detecting plasma enrichment of the stable isotope, suggesting a problem with the injection. One mouse was excluded from lipidomics analysis, due to low levels of all lipid species. Most experiments were not blinded, with the exception of plasma glucose in P2 pups (Fig. 1j), as the pups were not genotyped at the time the glucose was measured. We utilized Student's *t*-tests, 2-way analysis of variance, and Fisher's exact tests, as appropriate. *P* values below 0.05 were considered significant.

## Supplementary Material

Refer to Web version on PubMed Central for supplementary material.

## Acknowledgments

This work was supported by US National Institutes of Health grants HL111206 (R.A.H.), DK57539, DK58282 (D.A.), DK58132 (I.J.K.), DK45024 (R.G.-J.), and DK63608 (Columbia Diabetes Research Center), and DK020541 (Einstein Diabetes Research and Training Center). Additional support was from 3R37DK058282, a grant for Collaborative Activities to Promote Metabolomics Research (NOT-RM-11-024). M.A.F. is supported by a Senior Principal Research Fellowship (APP1021168) and Project Grant (APP1007465) from the National Health and Medical Research Council of Australia. We thank Rudy Leibel, UtpalPajvani, Alan Tall, Ira Tabas, as well as members of the Accili, Febbraio, and Kurland laboratories, for insightful discussion of the data. We acknowledge excellent technical support from A. Flete, T. Kolar and J. Lee.

## Abbreviations used

<b>B6</b>	C57BL/6J
<b>DG</b>	Diglyceride
<b>DNL</b>	De novo lipogenesis
<b>F–RF</b>	Fasting Refeeding
<b>HGP</b>	Hepatic glucose production
<b>HR–GTT</b>	Hepatic recycling glucose tolerance test
<b>G6pt</b>	Glucose 6-phosphate transporter (encoded by <i>Slc37a4</i> )
<b>RF</b>	Refeeding
<b>T2D</b>	Type 2 diabetes
<b>TG</b>	Triglyceride
<b>WTD</b>	Western type diet

## References

1. Brown MS, Goldstein JL. Selective versus total insulin resistance: a pathogenic paradox. *Cell Metab.* 2008; 7:95–96. [PubMed: 18249166]
2. Lin HV, Accili D. Hormonal regulation of hepatic glucose production in health and disease. *Cell Metab.* 2011; 14:9–19. [PubMed: 21723500]



3. Matsumoto M, Pocai A, Rossetti L, Depinho RA, Accili D. Impaired regulation of hepatic glucose production in mice lacking the fork head transcription factor Foxo1 in liver. *Cell Metab.* 2007; 6:208–216. [PubMed: 17767907]
4. Dong XC, et al. Inactivation of hepatic Foxo1 by insulin signaling is required for adaptive nutrient homeostasis and endocrine growth regulation. *Cell Metab.* 2008; 8:65–76. [PubMed: 18590693]
5. Lu M, et al. Insulin regulates liver metabolism in vivo in the absence of hepatic Akt and Foxo1. *Nat Med.* 2012; 18:388–395. [PubMed: 22344295]
6. Zhang K, et al. Hepatic suppression of Foxo1 and Foxo3 causes hypoglycemia and hyperlipidemia in mice. *Endocrinology.* 2012; 153:631–646. [PubMed: 22147007]
7. Haeusler RA, Kaestner KH, Accili D. FoxOs Function Synergistically to Promote Glucose Production. *J Biol Chem.* 2010; 285:35245–35248. [PubMed: 20880840]
8. Li S, Brown MS, Goldstein JL. Bifurcation of insulin signaling pathway in rat liver: mTORC1 required for stimulation of lipogenesis, but not inhibition of gluconeogenesis. *Proc Natl Acad Sci U S A.* 2010; 107:3441–3446. [PubMed: 20133650]
9. Porstmann T, et al. SREBP activity is regulated by mTORC1 and contributes to Akt-dependent cell growth. *Cell Metab.* 2008; 8:224–236. [PubMed: 18762023]
10. Yecies JL, et al. Akt stimulates hepatic SREBP1c and lipogenesis through parallel mTORC1-dependent and independent pathways. *Cell Metab.* 2011; 14:21–32. [PubMed: 21723501]
11. Gershman B, et al. High-resolution dynamics of the transcriptional response to nutrition in *Drosophila*: a key role for dFOXO. *Physiol Genomics.* 2007; 29:24–34. [PubMed: 17090700]
12. Haeusler RA, Pratt-Hyatt M, Welch CL, Klaassen CD, Accili D. Impaired generation of 12-hydroxylated bile acids links hepatic insulin signaling with dyslipidemia. *Cell Metab.* 2012; 15:65–74. [PubMed: 22197325]
13. Ido-Kitamura Y, et al. Hepatic FoxO1 Integrates Glucose Utilization and Lipid Synthesis through Regulation of Chrebp O-Glycosylation. *PLoS One.* 2012; 7:e47231. [PubMed: 23056614]
14. Tao R, et al. Hepatic FoxOs regulate lipid metabolism via modulation of expression of the nicotinamide phosphoribosyl transferase gene. *J Biol Chem.* 2011; 286:14681–14690. [PubMed: 21388966]
15. Zhang W, et al. FoxO1 regulates multiple metabolic pathways in the liver: effects on gluconeogenic, glycolytic, and lipogenic gene expression. *J Biol Chem.* 2006; 281:10105–10117. [PubMed: 16492665]
16. Haeusler RA, Han S, Accili D. Hepatic FoxO1 Ablation Exacerbates Lipid Abnormalities during Hyperglycemia. *J Biol Chem.* 2010; 285:26861–26868. [PubMed: 20573950]
17. Samuel VT, et al. Fasting hyperglycemia is not associated with increased expression of PEPCK or G6Pc in patients with Type 2 Diabetes. *Proc Natl Acad Sci U S A.* 2009; 106:12121–12126. [PubMed: 19587243]
18. Xiong X, Tao R, DePinho RA, Dong XC. Deletion of hepatic FoxO1/3/4 genes in mice significantly impacts on glucose metabolism through down regulation of gluconeogenesis and upregulation of glycolysis. *PLoS One.* 2013; 8:e74340. [PubMed: 24015318]
19. Li Y, Mechin MC, van de Werve G. Diabetes affects similarly the catalytic subunit and putative glucose-6-phosphate translocase of glucose-6-phosphatase. *J Biol Chem.* 1999; 274:33866–33868. [PubMed: 10567346]
20. Matschinsky FM. Assessing the potential of glucokinase activators in diabetes therapy. *Nat Rev Drug Discov.* 2009; 8:399–416. [PubMed: 19373249]
21. Velho G, et al. Impaired hepatic glycogen synthesis in glucokinase-deficient (MODY-2) subjects. *J Clin Invest.* 1996; 98:1755–1761. [PubMed: 8878425]
22. Postic C, et al. Dual roles for glucokinase in glucose homeostasis as determined by liver and pancreatic beta cell-specific gene knock-outs using Cre recombinase. *J Biol Chem.* 1999; 274:305–315. [PubMed: 9867845]
23. O'Doherty RM, Lehman DL, Telemaque-Potts S, Newgard CB. Metabolic impact of glucokinase overexpression in liver: lowering of blood glucose in fed rats is accompanied by hyperlipidemia. *Diabetes.* 1999; 48:2022–2027. [PubMed: 10512368]
24. Ferre T, Riu E, Bosch F, Valera A. Evidence from transgenic mice that glucokinase is rate limiting for glucose utilization in the liver. *Faseb J.* 1996; 10:1213–1218. [PubMed: 8751724]

25. Grimsby J, et al. Allosteric activators of glucokinase: potential role in diabetes therapy. *Science*. 2003; 301:370–373. [PubMed: 12869762]
26. Lloyd DJ, et al. Antidiabetic effects of glucokinase regulatory protein small-molecule disruptors. *Nature*. 2013; 504:437–440. [PubMed: 24226772]
27. Pfefferkorn JA, et al. The design and synthesis of indazole and pyrazolopyridine based glucokinase activators for the treatment of type 2 diabetes mellitus. *Bioorganic & medicinal chemistry letters*. 2012; 22:7100–7105. [PubMed: 23089526]
28. Hirota K, et al. A combination of HNF-4 and Foxo1 is required for reciprocal transcriptional regulation of glucokinase and glucose-6-phosphatase genes in response to fasting and feeding. *J Biol Chem*. 2008; 283:32432–32441. [PubMed: 18805788]
29. Iynedjian PB, Ucla C, Mach B. Molecular cloning of glucokinase cDNA. Developmental and dietary regulation of glucokinase mRNA in rat liver. *J Biol Chem*. 1987; 262:6032–6038. [PubMed: 3553185]
30. Walker DG, Holland G. The development of hepatic glucokinase in the neonatal rat. *Biochem J*. 1965; 97:845–854. [PubMed: 5883129]
31. Bossard P, Parsa R, Decaux JF, Iynedjian P, Girard J. Glucose administration induces the premature expression of liver glucokinase gene in newborn rats. Relation with DNase-I-hypersensitive sites. *European journal of biochemistry / FEBS*. 1993; 215:883–892. [PubMed: 8354293]
32. Xu J, et al. Decreased hepatic futile cycling compensates for increased glucose disposal in the Pten heterodeficient mouse. *Diabetes*. 2006; 55:3372–3380. [PubMed: 17130482]
33. Nissim I, et al. Effects of a glucokinase activator on hepatic intermediary metabolism: study with <sup>13</sup>C-isotopomer-based metabolomics. *Biochem J*. 2012; 444:537–551. [PubMed: 22448977]
34. Xu J, et al. Determination of a glucose-dependent futile recycling rate constant from an intraperitoneal glucose tolerance test. *Analytical biochemistry*. 2003; 315:238–246. [PubMed: 12689833]
35. Ferre T, Riu E, Franckhauser S, Agudo J, Bosch F. Long-term overexpression of glucokinase in the liver of transgenic mice leads to insulin resistance. *Diabetologia*. 2003; 46:1662–1668. [PubMed: 14614559]
36. Samuel VT, Shulman GI. Mechanisms for insulin resistance: common threads and missing links. *Cell*. 2012; 148:852–871. [PubMed: 22385956]
37. Shimomura I, et al. Decreased IRS-2 and increased SREBP-1c lead to mixed insulin resistance and sensitivity in livers of lipodystrophic and ob/ob mice. *Mol Cell*. 2000; 6:77–86. [PubMed: 10949029]
38. Sun Z, et al. Hepatic Hdac3 promotes gluconeogenesis by repressing lipid synthesis and sequestration. *Nat Med*. 2012; 18:934–942. [PubMed: 22561686]
39. Qiang L, Accili D. Uncoupling of acetylation from phosphorylation regulates FOXO1 function independent of its sub-cellular localization. *J Biol Chem*. 2010
40. Kitamura YI, et al. FoxO1 protects against pancreatic beta cell failure through NeuroD and MafA induction. *Cell Metab*. 2005; 2:153–163. [PubMed: 16154098]
41. Ozcan L, et al. Calcium signaling through CaMKII regulates hepatic glucose production in fasting and obesity. *Cell Metab*. 2012; 15:739–751. [PubMed: 22503562]
42. Bugianesi E, et al. Insulin resistance in non-diabetic patients with non-alcoholic fatty liver disease: sites and mechanisms. *Diabetologia*. 2005; 48:634–642. [PubMed: 15747110]
43. Monnier L, Colette C, Dunseath GJ, Owens DR. The loss of postprandial glycaemic control precedes stepwise deterioration of fasting with worsening diabetes. *Diabetes Care*. 2007; 30:263–269. [PubMed: 17259492]
44. Okamoto H, Obici S, Accili D, Rossetti L. Restoration of liver insulin signaling in Insr knockout mice fails to normalize hepatic insulin action. *J Clin Invest*. 2005; 115:1314–1322. [PubMed: 15864351]
45. Haas JT, et al. Hepatic insulin signaling is required for obesity-dependent expression of SREBP-1c mRNA but not for feeding-dependent expression. *Cell Metab*. 2012; 15:873–884. [PubMed: 22682225]

46. Vaitheesvaran B, et al. Peripheral effects of FAAH deficiency on fuel and energy homeostasis: role of dysregulated lysine acetylation. *PLoS One*. 2012; 7:e33717. [PubMed: 22442717]
47. Barber MN, et al. Plasma lysophosphatidylcholine levels are reduced in obesity and type 2 diabetes. *PLoS One*. 2012; 7:e41456. [PubMed: 22848500]

Author Manuscript

Author Manuscript

Author Manuscript

Author Manuscript

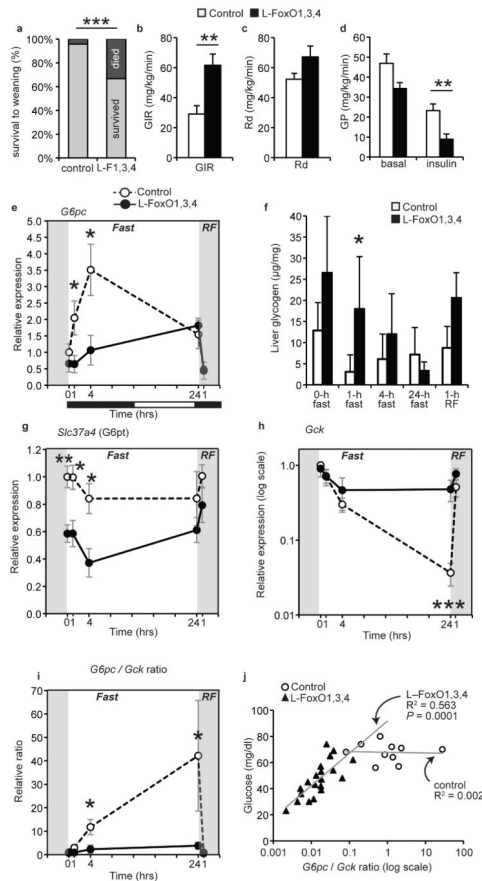


**Figure 1.**

Glucose parameters in L-FoxO1,3,4 mice. (a) Percentage of pups surviving to weaning at 21 days.  $n = 70$  control and 24 L-FoxO1,3,4 pups. \*\*\* $P < 0.001$  by Fisher's exact test. These numbers may underestimate the true mortality of L-FoxO1,3,4 pups; at genotyping (day 9) they are already present at less than Mendelian ratios<sup>7</sup>. (b-d) During hyperinsulinemic-euglycemic clamp ( $n = 8$  controls, 6 L-FoxO 1,3,4): (b) glucose infusion rate (GIR); (c) rate of glucose disposal (Rd); (d) glucose production (GP) \*\* $P < 0.01$  by Student's t test (2-tailed). (e-i) Liver gene expression and glycogen content during F-RF time course ( $n = 4-7$ , exact  $n$  for each time point and genotype listed in materials & methods): (e) *G6pc* expression; (f) liver glycogen; (g) *Slc37a4*, encoding the glucose 6-phosphate transporter; (h) *Gck*; (i) *G6pc/Gck*ratio. \*\*\*  $P < 0.001$ , \*\* $P < 0.01$ , \* $P < 0.05$  for control vs. L-FoxO1,3,4 mice by Student's t test (2-tailed). Black and white bars indicate the dark/light cycle. (j) Correlation between glucose levels and the *G6pc/Gck* ratio in pups at P2. Data are mean  $\pm$  s.e.m.

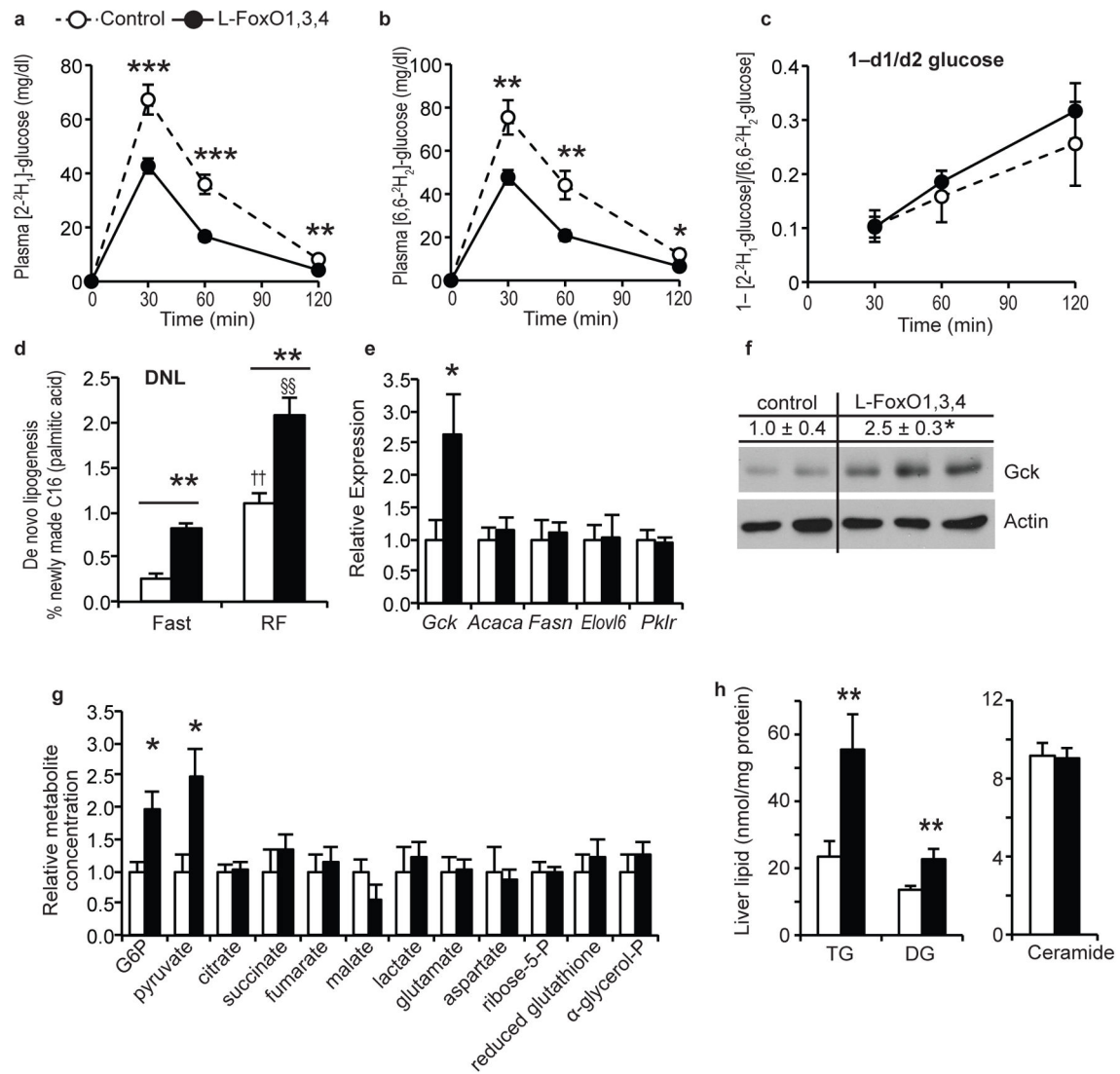


**Figure 2.**

Glucose utilization and lipogenesis. (a) Plasma levels of [2-<sup>2</sup>H<sub>1</sub>]-glucose after injection. (b) Plasma levels of [6,6-<sup>2</sup>H<sub>2</sub>]-glucose after injection. (c) Fractional difference in labeled glucose enrichment. (*n* = 9 control, 11 L-FoxO1,3,4). \*\*\**P* < 0.001, \*\**P* < 0.01, \**P* < 0.05 for control vs. L-FoxO1,3,4 mice, by Student's *t*-tests (2-tailed). (d) De novo lipogenesis. (*n* = 4 control, fasted; 5 L-FoxO1,3,4, fasted; 7 control, RF; 5 L-FoxO1,3,4, RF). \*\**P* < 0.01 for control vs. L-FoxO1,3,4 mice; ††*P* < 0.01 for RF vs. fasted control mice; §§*P* < 0.01 for RF vs. fasted L-FoxO1,3,4 mice by 2-way ANOVA. (e) Fasting gene expression (*n* = 7 control; 5 L-FoxO1,3,4). \**P* < 0.05. (f) Western blot of glucokinase in liver lysates from fasting mice (*n* = 4 control; 5-L FoxO1,3,4; representative blot shown). Numerical values above the blot are mean ±s.e.m. of Gck/actin, relative to controls. \**P* < 0.05. (g) Liver metabolites measured by GC-MS, relative to controls (*n* = 4 control; 5 L-FoxO1,3,4). \**P* < 0.05. (h) Liver lipidomic analyses. Total levels of the indicated lipid species. Full data set,

including individual lipid species available in Supplementary Table 1. ( $n = 14$  control; 11 L-FoxO1,3,4).  $**P < 0.01$  by Student's  $t$  tests (2-tailed).

Author Manuscript

Author Manuscript

Author Manuscript

Author Manuscript

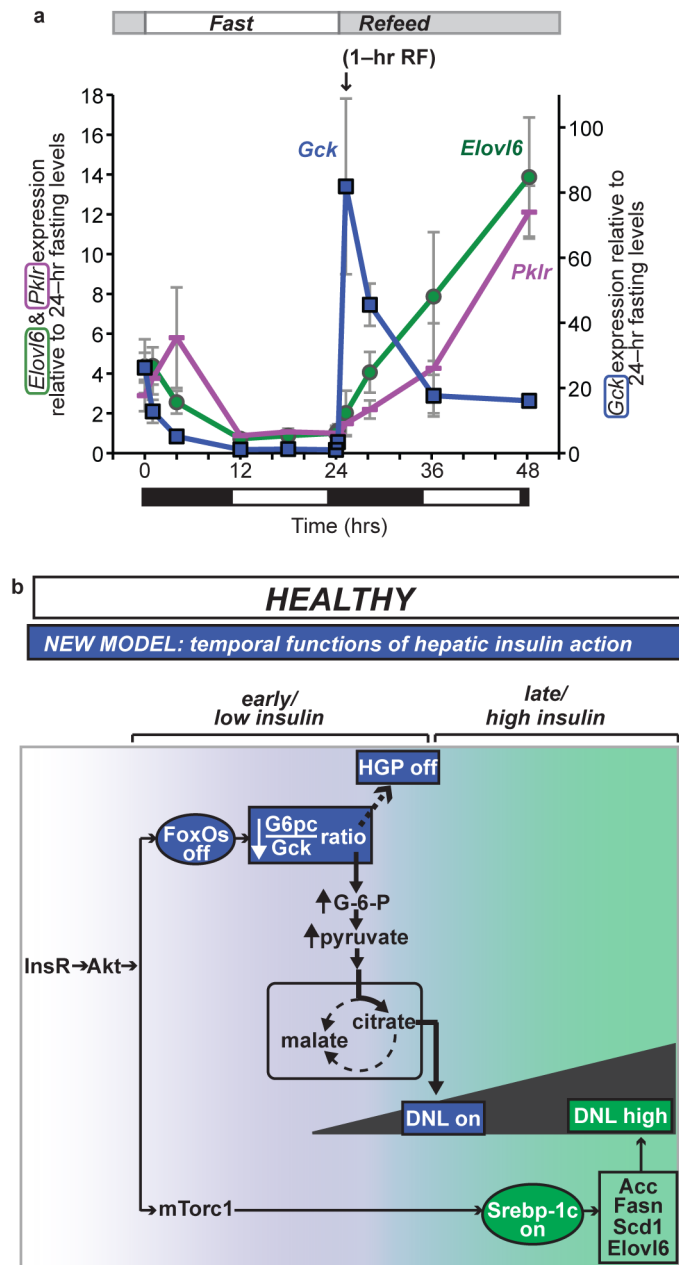


**Figure 3.** Lipogenic gene expression during F–RF in chow–fed C57BL/6J mice and proposed physiologic model (a) Comparison of *Gck*, *Elov16*, and *Pklr* expression. For each gene, the 24–hr fasting time point is set equal to 1. *Elov16* and *Pklr* are plotted using the vertical axis on the left, and *Gck* is plotted using the vertical axis on the right.  $n = 5$  per group. Black and white bars indicate the dark/light cycle. (b) Model. Earlier data suggested parallel action of insulin through FoxO to regulate HGP, and through Srebp–1c to regulate DNL. We propose a new model, whereby: insulin acts first at low levels and early time points through FoxOs to reduce HGP and initiate postprandial DNL by reducing the *G6pc*/*Gck* ratio; and second at high levels and late time points through Srebp–1c to amplify DNL.

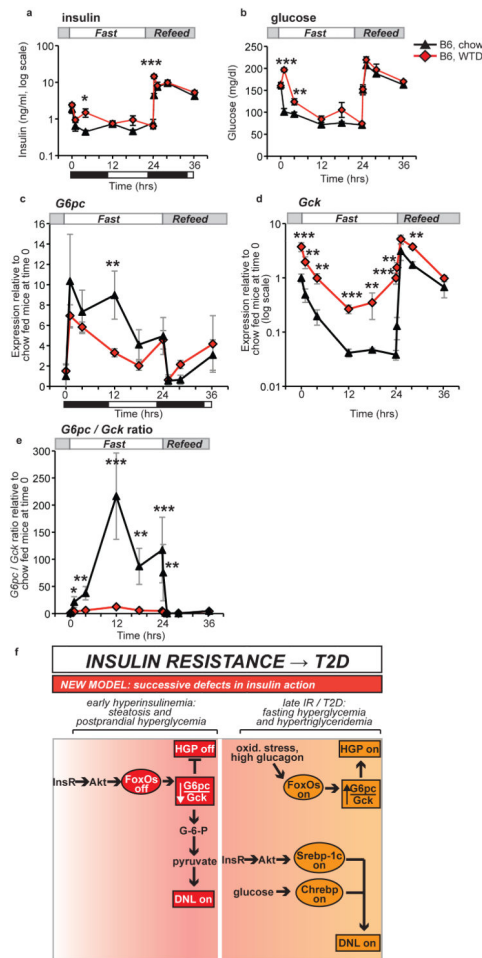


**Figure 4.** Pathophysiology and model. (a) Insulin and (b) glucose during F–RF in C57BL/6J mice fed chow or WTD for one week.  $n = 5$  per group. (c) *G6pc* expression (d) *Gck* expression (e) *G6pc/Gck* ratio from chow and WTD–fed C57BL/6J mice during F–RF. Expression in chow–fed mice at time 0 is set equal to 1.  $n = 5$  per group. Black and white bars indicate the dark/light cycle. \* $P < 0.05$ ; \*\* $P < 0.01$ ; \*\*\* $P < 0.001$  for chow vs. WTD–fed mice by Student’s *t* tests (2–tailed). (f) Model of the progression of insulin resistance and type 2 diabetes. The current model suggests bifurcation of insulin signaling, such that the FoxO branch is resistant to insulin and the Srebp–1c branch is excessively activated by hyperinsulinemia. We propose a new model, with successive defects in hepatic insulin action. In early hyperinsulinemia, FoxOs are strongly suppressed, thereby decreasing the *G6pc/Gck* ratio and activating lipogenesis. Later in disease progression, the Srebp–1c and Chrebp pathways are activated by insulin, whereas FoxOs may be activated by other mechanisms, e.g. oxidative stress induced acetylation or glucagon–induced alternative phosphorylation.